Roughness effects on sub-pixel radiant temperatures in kinetically isothermal surfaces

Iryna Danilina[1], Amit Mushkin[1], Alan Gillespie[1], Michael O'Neal[2], Lisa Pietro[2], Lee Balick[3]

1) University of Washington, 2) University of Delaware, 3) Los Alamos National Laboratory

Introduction. Temperature/emissivity estimation from remotely measured radiances generally assumes that scene elements represented by pixels in fact have a single emissivity spectrum and are isothermal. Thus, estimated temperatures and emissivities are effective values that would be found if these simplified assumptions were met. In reality, the physical scene is neither homogeneous nor isothermal, and the effective values are not strictly representative of the scene. How much in error are they? In this study we report on the dispersion of radiant temperature from the unresolved scene elements comprising a pixel due to roughness for the simple case when the scene actually is isothermal: i.e., the kinetic (but not radiant) temperature is everywhere the same.

Study area. Natural scenes used in the experiment were monolithologic expanses of bedrock and alluvial surfaces in the Mojave Desert, California. We studied ~0.5-m to ~ 10-m landscapes from four geographic sites.

Death Valley

Owens Valley

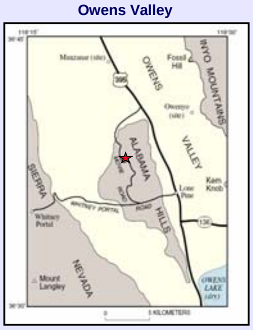

The Dogleg site is a 90º kink in a fluvial channel on Trail Canyon Fan on the west side of Death Valley. The Kit Fox site is from the alluvial fans below the Kit Fox Hills, on the east side of Death Valley. The Alabama Hills site is from the pediment near Movie Flats, west of the Alabama Hills in Owens Valley. The Mars Hill site is near Artist's Drive, on the east side of Death Valley

Data. High-resolution DTMs were generated from tripod-mounted LiDAR (Trimble GS-2000) measurements. We developed the radiosity model (form-factor approach) for predicting temperature effects due to scene roughness. Radiant temperature images were measured at various view angles using a FLIR broadband TIR camera (FLIR Systems Inc.) with NEΔT≈0.3 K.

Example of surface used: natural bedrock surface (Alabama Hills site, Owens Valley, California); surface size is 1.4 m by 2.5 m; DEM resolution is 3 cm; number of pixels = 4042.

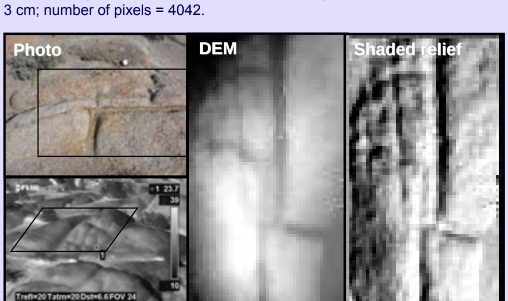

Example of surface used: alluvial fan surface (Kit Fox site, Death Valley, California); surface size is 0.6 m by 0.75 m; DEM resolution is 1 cm; number of pixels = 4636.

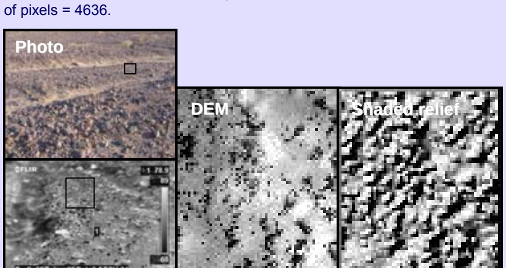

Radiosity model. The total radiance from the surface element, consisting of energy emitted by this surface element and the reflected energy of adjacent surface elements, is called radiosity, and models that predict it are called radiosity models. All surfaces were assumed Lambertian. The full radiosity model for TIR case is written as:

$$B_i = R_i + \rho \cdot \sum_{j=1}^{n} B_j \cdot F_{ij},\ i,j = 1,2 \ldots n,$$

where B_i – radiosity of a surface element i; R_i - thermal energy released from a surface element i; ρ – reflectivity of a surface element; F_{ji} - form factor from surface element j to surface element i; n – number of surface elements.

There are n unknown radiosities and n linear equations associated with individual pixels. Rearranging this equation, the n linear equations can be written in a matrix expression:

$$\begin{bmatrix} 1-\rho F_{11} & \cdots & -\rho F_{1n} \\ -\rho F_{21} & \cdots & -\rho F_{2n} \\ \vdots & & \vdots \\ -\rho F_{n1} & \cdots & 1-\rho F_{nn} \end{bmatrix} \cdot \begin{bmatrix} B_1 \\ B_2 \\ \vdots \\ B_n \end{bmatrix} = \begin{bmatrix} R_1 \\ R_2 \\ \vdots \\ R_n \end{bmatrix}$$

Surface radiance is given by

$$R = \varepsilon \cdot \int_{\lambda_1}^{\lambda_2} \frac{c_1}{\lambda^5} \cdot \frac{1}{e^{c_2/\lambda T} - 1} d\lambda,$$

where ε – emissivity of a surface; $c_1=3.74 \cdot 10^{-16}\ W\ m^2$ – first radiation constant; $c_2=0.0144\ m\ K$ – second radiation constant ; $\lambda_1=8 \cdot 10^{-6}\ m$, $\lambda_2=14 \cdot 10^{-6}\ m$ - lower and upper limits of the thermal part of the spectrum respectively.

The key step of the radiosity model is determining form factors. Form factor describes the radiance emitted from one point and incident on another:

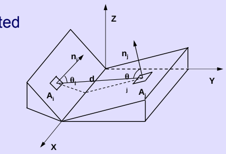

$$F_{ji} = \frac{\cos\theta_i \cdot \cos\theta_j}{d^2 \cdot \pi} \cdot A_i,$$

where F_{ji} – form factor from surface element j to surface element i; θ - projection angle between the normal of a surface element and line linking the pair of elements together; A_i – area of surface element i; d - the distance between two elements.

Model results

Alabama Hills site:

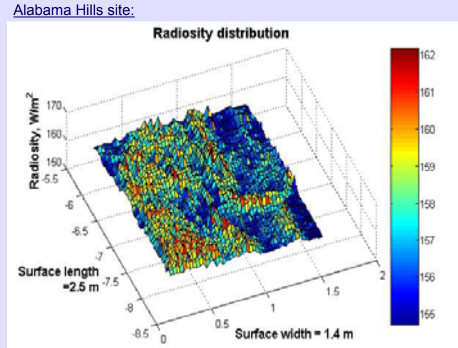

Kinetic temperature = 300 K; Surface emissivity = 0.9; Surface RMS = 0.084 m; Mean radiosity = 157.29 W m-2;Radiosity RMS = 1.48 W m-2;

Predicted effective temperature minus prescribed kinetic temperature : ΔT = 1.12 K;

Predicted emissivity minus prescribed emissivity: $\Delta\varepsilon$= 0.015.

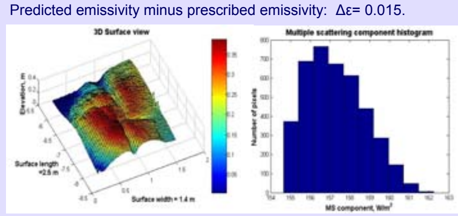

Kit Fox site:

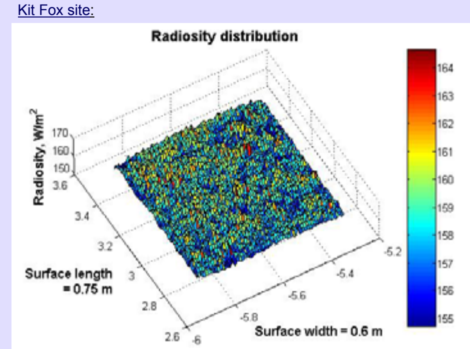

Kinetic temperature = 300 K; Surface emissivity = 0.9; Surface RMS = 0.027 m; Mean radiosity = 158.03 W m-2; Radiosity RMS = 1.49 W m-2;

Predicted effective temperature minus prescribed kinetic temperature : ΔT = 1.44 K;

Predicted emissivity minus prescribed emissivity: $\Delta\varepsilon$= 0.02.

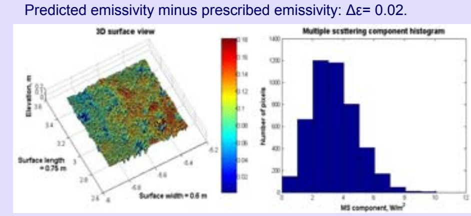

Effect of surface RMS on radiosity dispersion in alluvial scenes. The radiosity model results showed that, for isothermal alluvial surfaces, the radiosity dispersion increases with surface roughness.

Radiosity RMS vs. surface roughness:

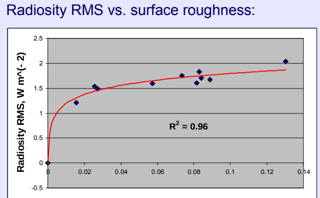

Predicted effective temperatures minus prescribed kinetic temperature (Delta T) vs. surface roughness:

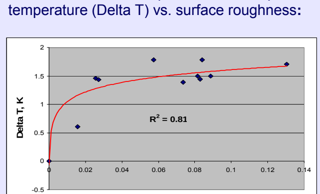

Conclusions. Radiant temperatures from complex surfaces vary because of reflection of energy from adjacent scene elements, added to the energy radiated in proportion to the kinetic temperature. The distribution of radiant temperature depends on the roughness and surface organization and is difficult to predict with simple statistical models that do not take into consideration the organization of surface roughness elements. The effective emissivity also varies because reflection and emission are complementary (cavity effect), and thus for very rough surfaces the emissivity approaches unity.

We have assumed for modeling that the kinetic temperature is everywhere the same, but this ideal condition is rarely realized in the field because some scene elements shadow others, because radiation of energy cools surfaces preferentially, established near-surface thermal gradients, and because of absorption of heat radiated from nearby slopes. It can be seen from our radiosity model that, even given our simplifying assumptions that minimize the effect, the disparity between effective temperatures from real ones is on the order of a few degrees, big enough to affect important TIR remote-sensing applications, such as energy-balance studies. For anisothermal surfaces, temperature dispersion is likely to increase with solar heating of exposed surface elements. It also follows that apparent emissivity will change over the course of the day, as cavities change from cooler to warmer than interstices.

We anticipate that, in the near future, dispersion of radiometric temperatures within a pixel will be measured over the course of a day, as sun-facing surfaces or surfaces with low thermal inertias are heated relative to their shadowed or high-inertia counterparts. Modeling based on these data should give a more realistic, quantitative estimate of the errors in recovered temperatures and emissivities due to surface roughness.